# The effects of tryptophan and hydrophobicity on the structure and bioactivity of novel indolicidin derivatives with promising pharmaceutical potential†

**Aaron P. Podorieszach and Heidi E. K. Huttunen-Hennelly***

***Received 12th October 2009, Accepted 22nd January 2010***
***First published as an Advance Article on the web 11th February 2010***
**DOI: 10.1039/b921248e**



In the current study, indolicidin, a known antimicrobial originally isolated from bovine neutrophils, was modified with respect to hydrophobicity and tryptophan content to maximize bioactivity, and minimize cytotoxicity. Since indolicidin contains five tryptophans (very hydrophobic) of its total 13 amino acids, alanine (mildly hydrophobic) was incrementally substituted in its place to generate five novel derivatives with decreasing hydrophobicity. Antimicrobial testing identified two active derivatives with minimum inhibitory concentrations in the $10^{-9}$ g mL$^{-1}$ range against *Candida albicans*, as well as broad-spectrum activity against various other Gram-positive/negative pathogens in the $10^{-3}$–$10^{-6}$ g mL$^{-1}$ range. Cytotoxicity testing yielded minimum hemolytic concentrations of ~$3 \times 10^{-3}$ g mL$^{-1}$ for both active derivatives, resulting in hemolytic indices of $>1.3 \times 10^{6}$ (peptide Δ45) and $3.6 \times 10^{5}$ (peptide Δ5) (improvements of >33 000-fold and ~10 000-fold, respectively, compared to indolicidin). The potent antimicrobial activity and low cytotoxicity of these derivatives show promise as potential antibiotics.

## Introduction

Antibiotics used to treat infection are rapidly becoming ineffective against a plethora of resistant pathogens, many of which are resistant to entire classes of drugs.[1] To combat this growing problem, researchers have been investigating new viable sources of drugs that are active against a broad spectrum of pathogens, safe, facile to synthesize and cost effective. One relatively novel class of such drugs is antimicrobial peptides (AMPs).

Although AMPs are relatively ubiquitous, occurring in species ranging from bacteria to humans, their mechanisms lend themselves to less resistance than commercial antibiotics because of their multiple modes of action.[2] Coined "dirty antibiotics", AMPs function through membrane permeabilization, intracellular targeting, and endotoxin neutralization, all of which give AMPs significant advantages over conventional antibiotics.[3] While AMPs can be designed *de novo*, it is often convenient to design structural analogues based off of natural AMPs, such as the peptide indolicidin (ILPWKWPWWPWRR-$NH_2$).

Originally isolated from bovine neutrophils, indolicidin is a 13-mer broad spectrum cationic AMP with a +3 overall charge and an amidated C-terminus.[4] Given the short nature of this peptide and the high proportion of tryptophan (38%) and proline (23%) residues, it has received attention as a potent antibiotic, yet its cytotoxic nature has demarcated its therapeutic use.[5]

Indolicidin derivatives have previously been created in an attempt to maximize antimicrobial activity and minimize hemolytic activity.[6] Indeed, the roles of both tryptophan[7] and proline[8] have been studied too, but there has not been any study that uses information from all the literature to generate a statistically-defined role of either of these two amino acids on bioactivity. Other studies may change the hydrophobicity by using unnatural amino acids,[9] but this may confound the results if the mechanism is stereoselective (such as through the use of a WPW protein-binding motif[10] or a 1-5-10 hydrophobic pattern for protein binding).[11] Furthermore, indolicidin has not been extensively tested against eukaryotic pathogens, such as *Candida albicans*, but it does seem to exert some activity against other fungal pathogens,[12] as well as protozoa,[13] HIV,[14] and other pathogens.[4] For these reasons, indolicidin was presently derivatized using incremental tryptophan substitutions for alanine, thereby decreasing the hydrophobicity of the AMP systematically and gradually. The synthesized derivatives (Table 1) were combined with current literature, and examined holistically.

## Results and discussion

Novel indolicidin derivatives were designed, synthesized and characterized to investigate the effects of tryptophan, and hydrophobicity on bioactivity. From there, the bioactive peptides were further characterized by determining hemolytic activity, and investigating secondary structure. Lastly, the mechanisms of action of the bioactive peptides were probed using a necrosis/apoptosis study.

**Table 1** Sequence of indolicidin (Δ0) and peptide derivatives with abbreviations

| Sequence of Designed Peptides | Abbreviations |
|---|---|
| ILPWKWPWWPWRR-$NH_2$ | Δ0 |
| ILPWKWPWWP **A**RR-$NH_2$ | Δ5 |
| ILPWKWPW **AP A**RR-$NH_2$ | Δ45 |
| ILPWKWP **A AP A**RR-$NH_2$ | Δ345 |
| ILPWK **AP A AP A**RR-$NH_2$ | Δ2345 |
| ILP **AK AP A AP A**RR-$NH_2$ | Δ12345 |

Note: Single-letter amino acid abbreviations include: isoleucine (I), leucine (L) proline (P), tryptophan (W), arginine (R), and alanine (A).

*Department of Chemistry, Thompson Rivers University, 900 McGill Road, Kamloops, BC, Canada V2C 5N3; Tel: (+1) (250)377-6063. E-mail: hhuttunen@tru.ca*

† Electronic supplementary information (ESI) available: Mass spectra and HPLC traces. See DOI: 10.1039/b921248e

**Table 2** MICs of peptide derivatives against a variety of bacterial and fungal pathogens, where active concentrations are determined by exhibiting at least 90% reduced optical density compared to each control culture incubated without peptide; a dash (—) indicates that the peptide was not active at the concentrations tested

| | Active Concentration/g mL$^{-1}$ | | | | |
|---|---|---|---|---|---|
| Peptide | *Escherichia coli* | *Pseudomonas aeruginosa* | *Salmonella typhimurium* | *Candida albicans* | Methicillin-Resistant *Staphylococcus aureus* |
| Indolicidin | $2 \times 10^{-4}$ | $1 \times 10^{-4}$ | $2 \times 10^{-4}$ | $2 \times 10^{-4}$ | $1 \times 10^{-4}$ |
| Δ12345[a] | — | — | — | — | — |
| Δ2345[a] | — | — | — | — | — |
| Δ345[a] | — | — | — | — | — |
| Δ45 | $2 \times 10^{-4}$ | $4 \times 10^{-5}$ | $2 \times 10^{-5}$ | $2 \times 10^{-9}$ | $2 \times 10^{-5}$ |
| Δ5 | $5 \times 10^{-6}$ | — | $5 \times 10^{-6}$ | $8 \times 10^{-9}$ | $8 \times 10^{-5}$ |

[a] Peptides tested at concentrations from $1 \times 10^{-3}$ with ten-fold dilutions to $1 \times 10^{-9}$ g mL$^{-1}$



## Bioactivity

After subjecting the peptides to various antimicrobial assays, the minimum inhibitory concentrations (MICs) listed in Table 2 were determined.

A 90% cutoff for antimicrobial activity was used to demonstrate the inhibition of growth, rather than the concentrations at which the pathogens were actually lysed. In many instances, for example, higher concentrations of peptides caused complete solubilization of the cell membranes, leading to a 100% decrease in $OD_{600}$, whereas at lower concentrations near the MIC, growth was severely limited by over 90%, yet the initial inoculum often remained intact, yielding a slight absorbance. Moreover, this initial inoculum still remained viable, as demonstrated by reinoculating the pathogens in peptide-free media. Hence, this demonstrated a bacteriostatic concentration rather than a bacteriolytic concentration.

Growth inhibition without disrupting membrane integrity would also be indicative of an intracellular mechanism of action, which may be related to the hydrophobicity of the peptide derivatives. Indolicidin itself already has demonstrated protein-binding[11] and DNA-binding capabilities at levels below the critical membrane disrupting concentrations.[10] Given indolicidin's natural hydrophobic nature, it seems unlikely to cross the cell membrane; however, Hsu *et al.* demonstrate a remarkable molecular plasticity through indolicidin's numerous conformations in several cellular mimetic environments, ranging from a globular aqueous form (to minimize the hydrophobic tryptophan interactions with water) to a stretched conformation (to span the membrane), and a wedge shape that interacts with the membrane interface (tryptophan residues are, in particular, known for orienting themselves at membrane interfaces).[10a,b] Therefore, these numerous conformational changes appear to be necessary for the antimicrobial action of indolicidin (to gain access to intracellular targets), but these conformational changes also carry an energy burden. To facilitate these changes, it was hypothesized that reducing the hydrophobicity of several indolicidin derivatives would minimize the energy required to pass through the hydrophilic head groups of the cell membrane and would also shift the equilibrium of indolicidin's membrane interaction to favour dissociation from the cell membrane into the cytosol (Fig. 1).

As shown, indolicidin has a high membrane concentration with very little dissociating into the cytosol due to its higher hydrophobicity. The derivatives Δ45 and Δ5 may have been active for the following reason. The removal of one or two tryptophan residues

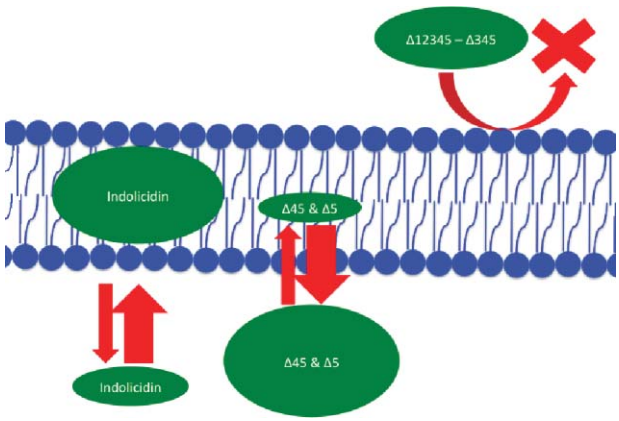


**Fig. 1** Hypothesized differences in mechanism between indolicidin and the derivatives synthesized in the present study.

decreased the net hydrophobicity of the peptide, facilitating its movement through the phospholipid bilayer into the cytosol. Conversely, derivatives Δ12345–Δ345 may not have been active due to their excessive reductions in hydrophobicity, becoming unable to pass through the hydrophobic cell membrane fatty acyl tails. On the other hand, reduction of three tryptophan residues may have affected the intracellular mode of action, noting the reduction in indole rings of the tryptophan residues, which may play a role in DNA-binding. Moreover, indolicidin has two WPW motifs, which have been shown to bind calmodulin, and may play a part in the intracellular mechanism of indolicidin.[11] Therefore, the removal of up to two tryptophan residues from the amidated C-terminus causes destruction of only a single WPW motif, whereas removal of three tryptophans causes destruction of the second WPW motif. Thus, there may have been some reduction in a protein-dependent intracellular mechanism with the derivatives Δ12345–Δ345. To elucidate which of these possibilities resulted in the loss of activity of Δ12345–Δ345, both protein binding potential (Boman Index) and net hydrophobicity were examined in a variety of indolicidin derivatives from literature, all of which had only been modified at tryptophan residues, keeping all other variables constant. The plot of the Boman index *vs.* antimicrobial activity is given in Fig. 2, while hydrophobicity *vs.* antimicrobial activity is given in Fig. 3. Hydrophobicity was calculated using the Wimley–White scale for peptides.[15] The Boman index is defined as "the sum of the free energies of the respective side chains for transfer from cyclohexane

 

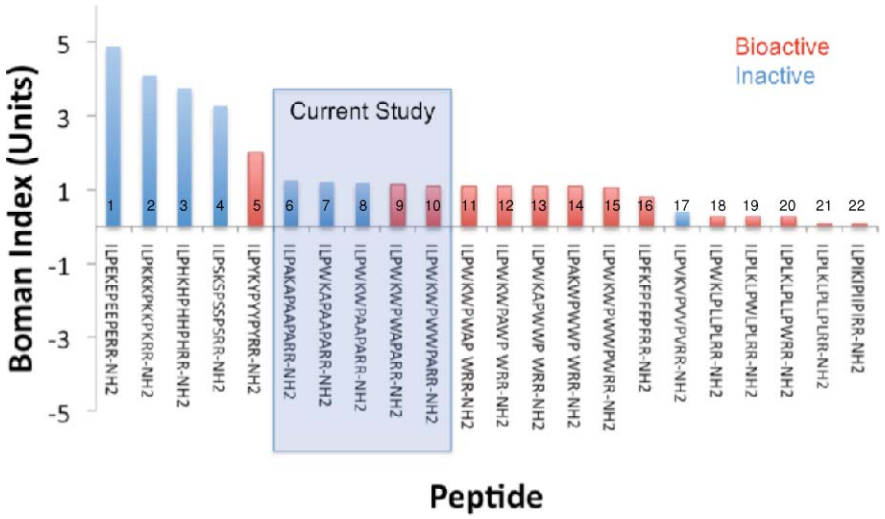


**Fig. 2** Protein-binding potentials of indolicidin tryptophan-substituted derivatives using the Boman index with active AMPs shown in red and inactive derivatives in blue; derivatives, numbered from left, include (1–5, 11–14, 16–17, 21–22),[8] 6–10 (current study), 15 (indolicidin), and 18–20.[7b]

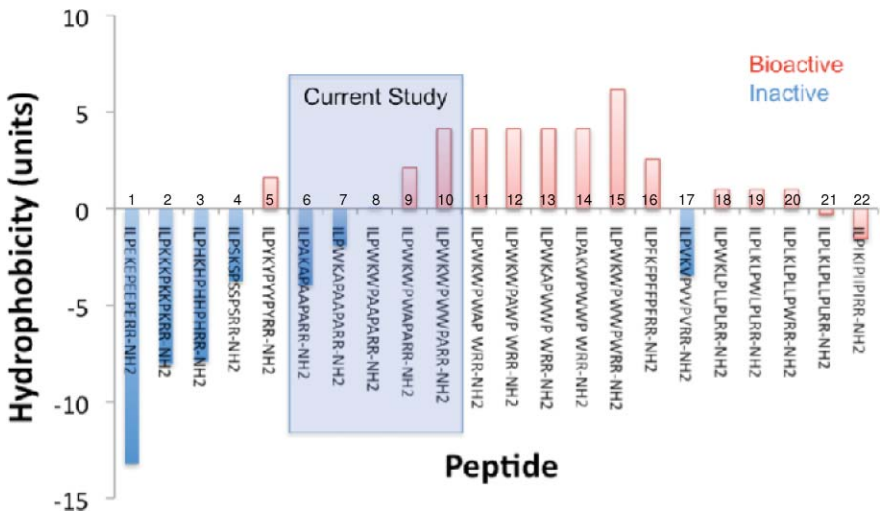


**Fig. 3** Hydrophobicity of indolicidin tryptophan-substituted derivatives using Wimley-White scale of hydrophobicity for peptides with active AMPs shown in red and inactive derivatives in blue; derivatives, numbered from left, include (1–5, 11–14, 16–17, 21–22),[8] 6–10 (current study), 15 (indolicidin), and 18–20.[7b]

to water… divided by the total number of the residues of an antimicrobial peptide. The calculated values are negative, but the + and – are reversed".[16]

It is worth mentioning that these graphs each demonstrate simple activity relationships (*i.e.* active/not active), but do not specify *how* active any given peptide is. Indeed, it appeared as though hydrophobicity was a significant variable ($P < 0.01$) in determining if a peptide would be active or not; however it was not indicative of any minimum inhibitory concentration. Perhaps the protein-binding potential becomes more of an activity determinant once the peptide is already in the cell, where then a high protein-binding affinity might be beneficial (binds to a target more strongly) or detrimental (binds non-specifically to random proteins).[16] Therefore, the protein-binding effects may be variable and appear to be less significant than the effects of hydrophobicity.

## Hemolysis

With respect to the cytotoxicity of the derivatives, each subsequent tryptophan substitution seemed to reduce hemolysis (Table 3). While it has been previously stated that tryptophan contributes to hemolytic but not antimicrobial activity,[7] it appears that tryptophan is involved in both. This is likely due to the dual roles of tryptophan as both a significant contributor to hydrophobicity/membrane-interface positioning and protein/DNA-binding. This provides an insight into the hemolytic nature of many cationic AMPs, where the specific mechanisms of self-promoted uptake through electrostatic associations with bacterial/fungal cell wall and lipopolysaccharide (LPS) components may only be one of the mechanisms of membrane interaction. In this particular case, hydrophobicity and tryptophan

**Table 3** Minimum hemolytic concentrations (MHCs) of indolicidin derivatives compared to native indolicidin. In cases of high MHCs, the highest concentration tested is given with its percent hemolysis at that concentration. Hemolytic Index (HI) is defined here as the MHC divided by the lowest MIC derived

| Peptide | Minimum hemolytic concentration/g $mL^{-1}$ | Hemolytic index (MHC/MIC) |
|---|---|---|
| Δ12345 | $>6.8 \times 10^{-3}$ (1%) | N $A^{-1}$ |
| Δ2345 | $>6.4 \times 10^{-3}$ (0%) | N $A^{-1}$ |
| Δ345 | $>6.7 \times 10^{-3}$ (17%) | N $A^{-1}$ |
| Δ45 | $>2.6 \times 10^{-3}$ (51%) | $>1.3 \times 10^{6}$ |
| Δ5 | $2.8 \times 10^{-3}$ | $3.6 \times 10^{5}$ |
| Indolicidin | $3.0 \times 10^{-5}$ | 39 |

membrane-interface propensity are likely both generalized mechanisms of membrane interaction with microbial and host cells. Therefore, by reducing the number of tryptophan residues in indolicidin, there may have been a relative decrease in the hemolysis because of the reduced hydrophobicity, and overall membrane-interface propensity of the peptide, while still maintaining the cationic specificity for microbial species. After further removal of tryptophan, there was virtually no hemolysis, even at high concentrations, but there was also less antimicrobial activity for the reasons discussed earlier.

Of particular interest in Table 3 are the hemolytic indices (HIs) of the derivatives compared to indolicidin. With respect to the lowest MIC value, it seems that Δ45 and Δ5 have dramatically improved therapeutic utility, especially against *C. albicans*. With improvements of approximately 10 000–33 000 in the HI, this gives these new derivatives an extremely large concentration range of safe activity, especially noting the facility of applying AMPs as topical treatments, such as those involved in the normal treatment of *C. albicans*.

Indolicidin, along with many AMPs, is known to bind LPS.[17] This gives AMPs an intrinsic secondary benefit, in that they may prevent disseminated intravascular coagulation when administered intravenously, compared to other conventional antibiotics, which may lyse bacteria, causing endotoxin release and endotoxic shock. While the LPS-binding properties of the derivatives are unknown (future work with capillary electrophoresis), it is likely that they are similar to indolicidin, noting broad spectrum activity against both Gram-negative and Gram-positive bacteria, as well as fungi. Along with an LPS-binding study, the novel derivatives should also be tested for regular membrane affinity to confirm any hypotheses about the causes of red blood cell hemolysis.

### Circular dichroism (CD) spectroscopy

CD spectroscopy is regularly used to quantify the extent of secondary structure present in peptides and proteins.[18] Peptides or proteins lacking well-defined three-dimensional structures produce little or no signal in the near-UV (250–350 nm) spectral region due to the time-averaged fluctuating structures.[19] Enhanced near-UV signals, on the other hand, are indicative of a well-defined structure due to the asymmetric environments of their aromatic chromophores.[20]

The samples were analyzed in phosphate buffer, as well as, in phosphate buffer with 50% TFE. The buffer–TFE solvent is both structure promoting and serves to mimic the membrane environment. The CD spectra of the bioactive peptides are shown in Fig. 4.

The CD spectra of the peptides were similar in both the aqueous and TFE conditions, respectively. No significant secondary structural changes with respect to indolicidin were observed for the alanine-based derivatives. Furthermore, all CD spectra suggest a lack of secondary structure (unordered), consistent with the findings of White and coworkers,[21] which is expected considering

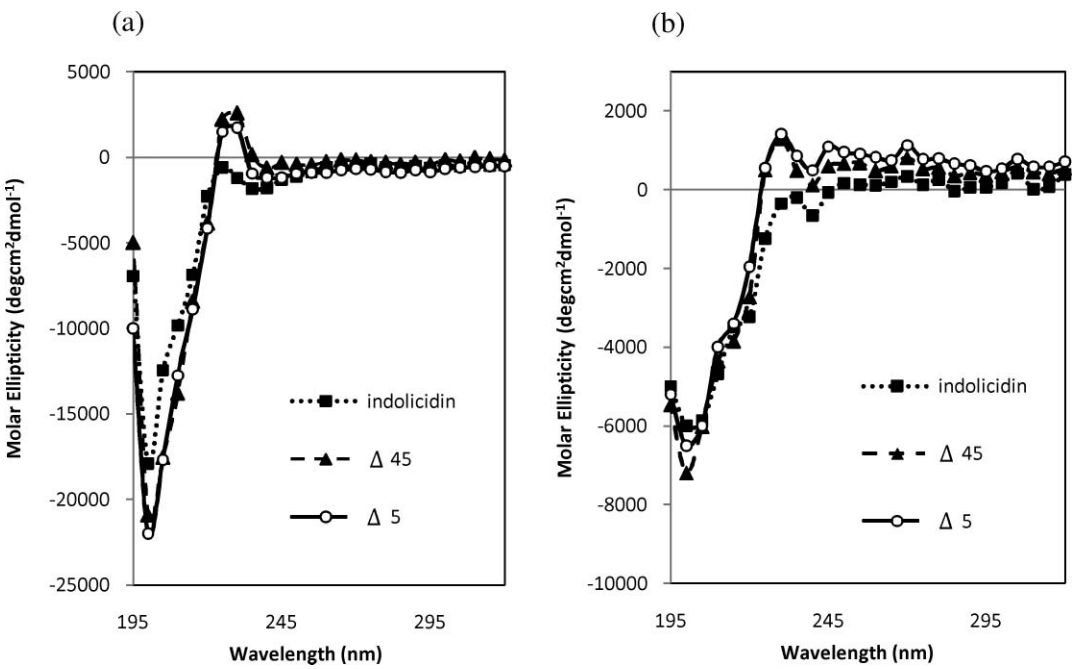


**Fig. 4** CD spectra of bioactive peptides at ~50 μM in aqueous (a) and TFE (b) environments recorded in 50 mM sodium phosphate buffer (pH 7.0) at 20 °C.

 

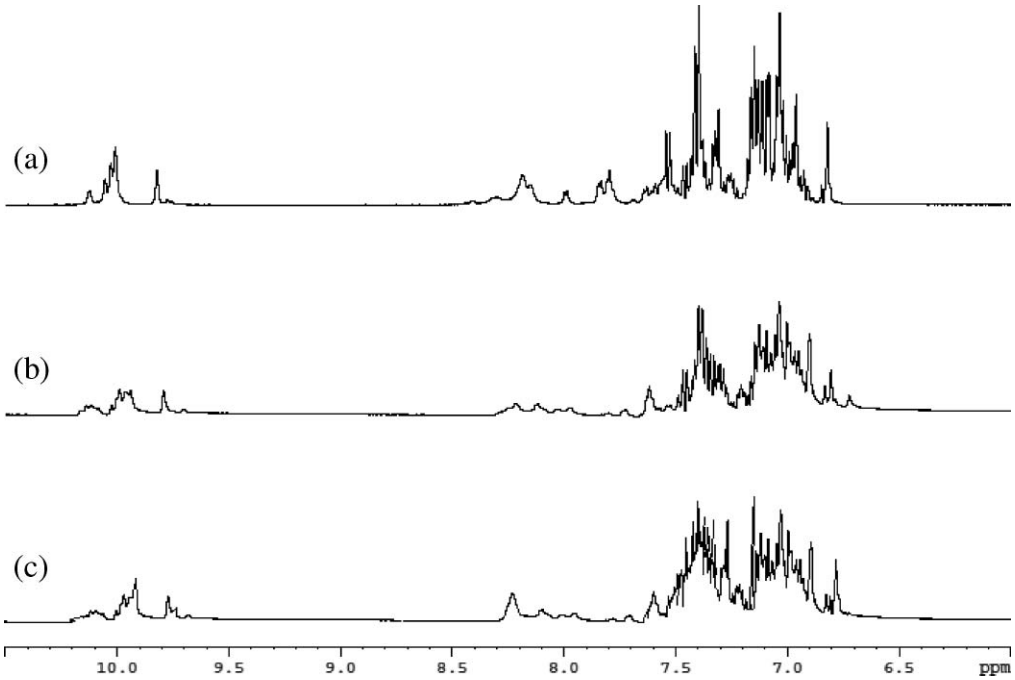


**Fig. 5** Expansions of the amide regions of 500 MHz $^1$H NMR spectra of the active peptides at ~1.5 mM in 10% $D_2O$, 45 mM phosphate buffer, pH 7.0 at 20 °C. (a) Δ45, (b) Δ5, (c) Δ0 indolicidin.

each of the peptides have three proline residues in their sequences. While indolicidin itself has been shown to be unordered in most solvents,[21] the removal of Trp residues may reduce steric hindrance and enable α-helical or β-sheet formation, although no change in secondary structure was observed for any of the active indolicidin derivatives.

### $^1$H NMR spectroscopy

One-dimensional $^1$H NMR spectroscopy is a simple diagnostic method used to investigate protein structure. The spectral region between 7 and 11 ppm is typically examined because distinct sharp and disperse signals are observed for native-like proteins corresponding to the slowly exchanging amide protons.[22] A stacked plot of the amide regions of the $^1$H NMR spectra for the bioactive peptides is shown in Fig. 5.

While there was significant overlap in the fingerprint regions of these spectra (<8.5 ppm), there was high enough resolution to see the Trp NH signals, which were shifted extremely downfield (~10 ppm) because of the deshielding effects of the indole rings. The number of signals in this region, however, was greater than the number of indole protons, indicating that these peptides sampled multiple conformations in aqueous solution, resulting in separate signals for each different conformation. Thus, broad and overlapping signals were indicative of a highly plastic molecule, which correlates well to the results of Hsu *et al.*,[10a,b] and to the CD spectra in Fig. 4 which indicate a lack of secondary structure.

### Necrosis/apoptosis

To further elucidate the mechanisms of action of the new derivatives, as well as to better characterize their potential cytotoxicity, the peptides were subjected to a necrosis/apoptosis assay (Sigma Apoptosis Kit). This kit functions on two basic principles. Firstly, AnnCy3 binds phosphatidylserine, which is normally only present on the inner leaflet of cell membranes in viable cells. In apoptotic cells, however, the membrane lipids flip phosphatidylserine to the outer membrane leaflet. In addition, in necrotic cells, the membrane is compromised and so AnnCy3 also has access to phosphatidylserine. Therefore, in both apoptotic and necrotic cells, AnnCy3 has access to phosphatidylserine, yielding a red fluorescence, whereas viable cells will not fluoresce. The second principle relies on 6-CFDA, which is membrane permeable until it passes into a cell, where it is cleaved by cellular esterases, thereby becoming impermeable and fluorescing green. In membrane-compromised necrotic cells, both the esterases and the membrane-impermeable green fluorescent stain leak out of the cell, resulting in no fluorescence. Conversely, in apoptotic and viable cells, the membrane remains intact, resulting in green fluorescence. Overall, apoptotic cells fluoresce both green and red, necrotic cells fluoresce red, and viable cells fluoresce green. Fig. 6 shows representative fluorescent images of Δ5 (images for Δ45 are similar and not shown).

As demonstrated in Fig. 7 and 8, there appears to be some effects on the nucleated animal cells that were not immediately obvious from the hemolysis test.

Indeed, in Fig. 7, there appears to be some concentration-dependent relationship between Δ45 and apoptosis/necrosis induction. At concentrations of $1.4 \times 10^{-4}$ g mL$^{-1}$ to $1.4 \times 10^{-5}$ g mL$^{-1}$, there appears to be a large increase in necrosis relative to the control, but at lower concentrations, there does not appear to be any significant difference compared to the control. At the highest concentration tested, however, there was actually a surprising shift

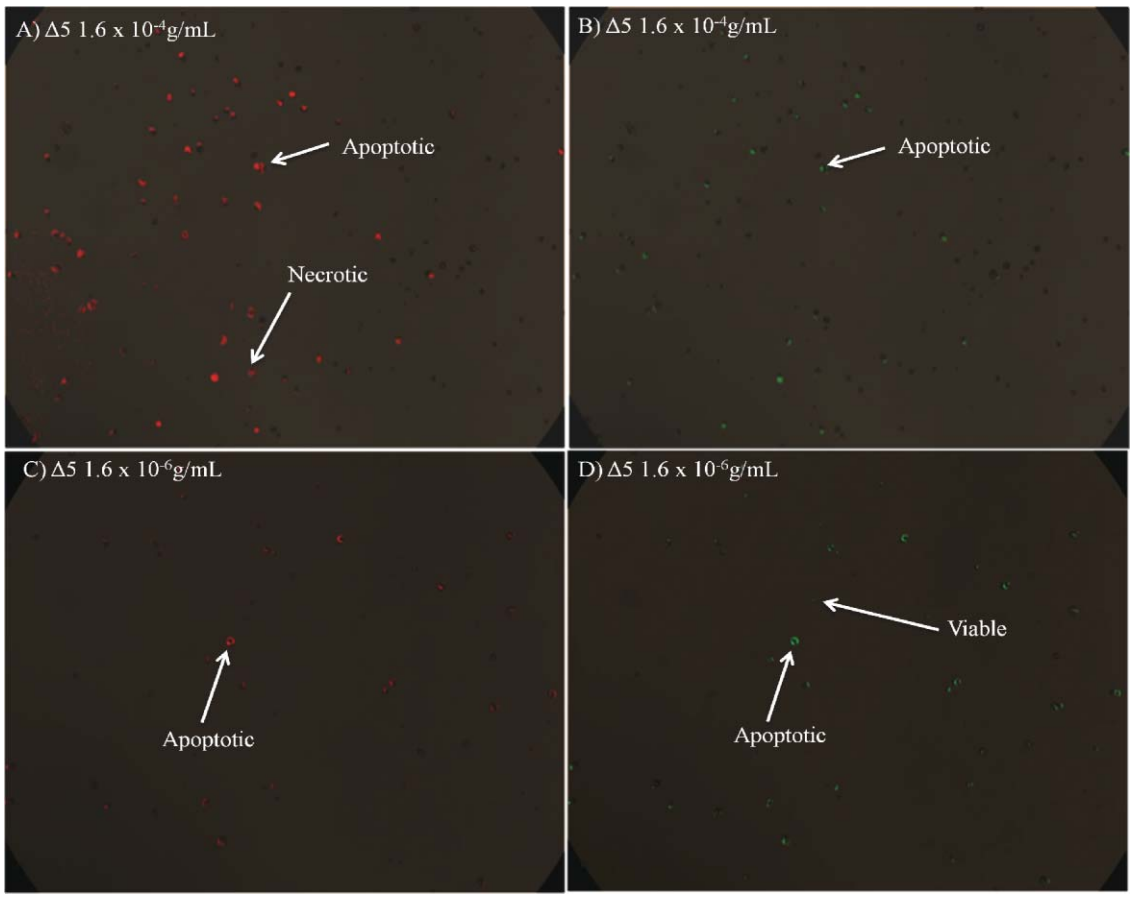


**Fig. 6** Fluorescent microscope images of peptide Δ5 at concentrations (A) and (B) $1.6 \times 10^{-4}$ g mL$^{-1}$ and (C) and (D) $1.6 \times 10^{-6}$ g mL$^{-1}$. The images were overlayed with brightfield microscopy, where figures (A) and (C) were observed with a red filter and (B) and (D) were observed with a green filter.

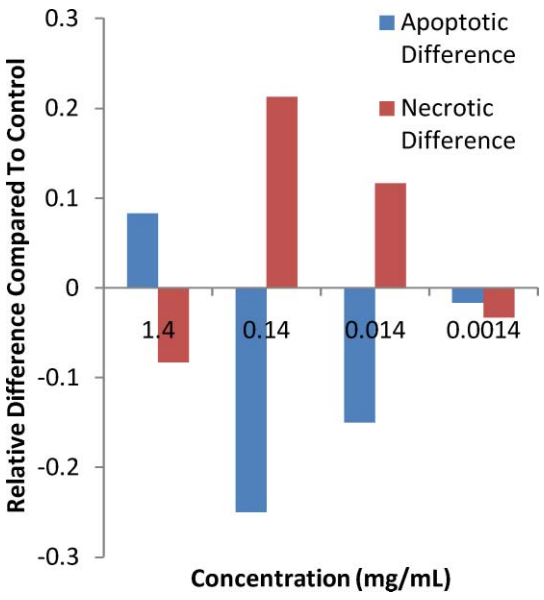


**Fig. 7** Changes in relative amounts of necrosis and apoptosis after treatment with peptide Δ45 and visualization using fluorescence microscopy with a Sigma Apoptosis Kit.

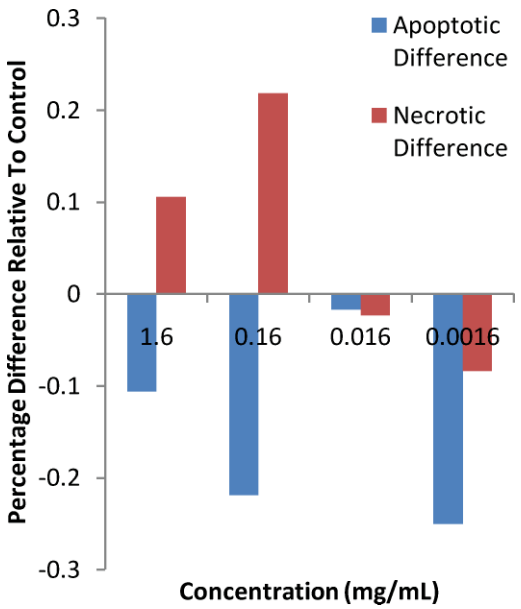


**Fig. 8** Changes in relative amounts of necrosis and apoptosis after treatment with peptide Δ5 and visualization using fluorescence microscopy with a Sigma Apoptosis Kit.

towards apoptosis induction. This was likely a result of the peptide reaching a high enough intracellular concentration to permeabilize either the nucleus (causing DNA degradation by DNAses) or mitochondrial permeabilization (causing release of cytochrome

 

C), both of which trigger the caspase cascade, leading to apoptosis. Conversely, Fig. 8 indicates that Δ5 acts in a similar concentration-dependent manner, causing necrosis from $1.6 \times 10^{-3}$ g mL$^{-1}$ to $1.6 \times 10^{-4}$ g mL$^{-1}$. There does not appear to be any significant difference between the control and Δ5 at $1.6 \times 10^{-5}$ g mL$^{-1}$, and at lower concentrations ($1.6 \times 10^{-6}$ g mL$^{-1}$), both apoptosis and necrosis were reduced as more cells remained viable.

## Conclusions and future work

Of the five derivatives synthesized, two showed substantially increased antimicrobial activity and decreased cytotoxicity compared to the parent AMP indolicidin, with a total of ~10 000-fold and >33 000-fold improvements in the HIs for peptides Δ5 and Δ45, respectively. The contribution of hydrophobicity to antimicrobial and hemolytic activity showed a significant relationship, whereas the direct effects of tryptophan remain ambiguous. To determine these effects, a native polyacrylamide gel electrophoresis DNA-binding study would be required to investigate any DNA-related mechanism of action. Biochemical characterization using CD and $^1$H NMR spectroscopy supported an absence of any secondary structure for indolicidin and its active derivatives in different cellular-mimetic solvents. Given the similar unordered structures of native indolicidin and its active derivatives, it seems that an intracellular mechanism is likely. Because of the cationic nature and presence of indole rings, DNA-binding is possible, but protein-binding may also play a significant role. Both these effects are contingent on the peptide's ability to penetrate through the outer membrane, where the active derivatives contained lower net hydrophobicity (yet still retaining a minimum level of hydrophobicity), facilitating their membrane transience and increasing their contact with intracellular targets. Given the intracellular targeting and the particular potency against eukaryotic *Candida albicans*, an apoptosis/necrosis kit was used to ensure safety against nucleated animal cells (where enucleated red blood cells in a hemolysis test would not be indicative of many of the organelle/nucleus-dependent mechanisms of action of cytotoxicity). It appeared that the derivatives were still safe at levels approaching the MHC, where, at this concentration, they caused significant amounts of apoptosis. This was indicative of membrane transience and activation of intracellular apoptosis signal cascades *via* mitochondrial disruption or DNA damage. Further research would be needed to determine the exact reason for this initiation of apoptosis; however, the concentration at which this occurs is substantially higher than the MIC, and therefore, there appears to be very little risk associated with the active derivatives. Moreover, the activity against *Candida albicans* is particularly useful since AMPs are facile to apply to topical infections, giving this peptide promising pharmacological potential. Furthermore, since our indolicidin derivatives exhibit good membrane transience, it would be interesting to see if they could penetrate biofilms (such as in the oral cavity). The peptides had high therapeutic indices and thus the MICs could be increased a hundred fold without any adverse effects (biofilm MICs normally ten to a hundred times higher than normal MICs). These peptides could be, for example, then included in a mouthwash product. As mentioned, the peptides were highly active against *C. albicans*, the common pathogen of oral thrush, and thus have significant potential for combating oral infections.

While the bioavailability of intravenous drugs is substantially less than orally administered drugs, further modifications to lower reduce the clearance of these derivatives could include (but are not limited to) cyclization, employment of unnatural or D/L amino acids, and terminal modifications. Further biochemical characterization should include the determination of the octanol–water coefficients to predict the distribution of the drug in the body and a capillary electrophoresis binding study of the derivatives' abilities to bind both LPS and phospholipid membranes to better understand the mechanisms of antimicrobial and hemolytic action, respectively.

## Experimental

### General

All reagents for the peptide syntheses were reagent grade. To confirm peptide identity, each active derivative was analyzed by mass spectroscopy and run on a Perspective Biosystems Voyager Elite MALDI-TOF MS operating in reflectron mode with delayed extraction using 50 μM cinnamic acid in 1 : 1, $H_2O$ : MeCN, as a matrix. A protein concentration kit (Bio-Rad) and Bradford Assay[23] protocol were used to determine peptide concentrations using a colorimetric assay. Absorbance was measured at 750 nm using a Cary UV/Vis spectrophotometer. Concentration was determined by linear interpolation to a calibration curve against bovine serum albumin. The pH's of the buffers were determined using a VWR SympHony SB90M5 pH meter calibrated with two purchased buffer standards (pH = 4.0 and 10.0).

### Peptide synthesis & purification

Peptides were synthesized by standard Fmoc chemistry using an Applied Biosystems 431A automated peptide synthesizer. The peptides were synthesized on a 0.25 mmol scale using the *FastMoc*™ protocols and all Fmoc protected amino acids, solvents and coupling reagents were purchased from Advanced Chemtech (Louisville, KY, USA). A single amino acid coupling cycle was approximately 55 min and included a: (1) Fmoc deprotection using piperidine, (2) washing using *N*-methylpyrrolidone (NMP), (3) coupling step to 1.0 mmol of the next Fmoc amino acid using 2-(1*H*-benzotriazole)1,1,3,3-tetramethyluronium hexafluorophosphate (HBTU) and 1-hydroxybenzotriazole (HOBt) as coupling reagent and lastly (4) wash with NMP. The peptides were then cleaved from the solid phase using a cleavage mixture (82.5% TFA; 5% thioanisole; 5% phenol; 5% water; 2.5% EDT) for 8 h at room temperature (the reaction was initially cooled in an ice bath for 10 min). Cleavage from the Rink[24] resin solid phase yielded an amidated C-terminus. The mixture was filtered through a medium-pore glass fritted filter and washed with DCM. The TFA and DCM were removed by rotary evaporation and the peptide was redissolved in water. Some impurities were removed by extraction into diethyl ether. Final purification of the peptides was performed using a Waters PrepLC 4000 system (250 mm × 21.20 mm × 10 μm particle size, 300 Å pore size) C18 reversed-phase column with 5 mL sample injections with detection at 220 nm (amide chromophore) and manual collection. The samples were filtered through a 0.45 μM Nylon™ syringe filter (Phenomenex) prior to injection, and run at a flow rate of 10 mL min$^{-1}$

**Table 4** % Yields and MALDI-MS characterization of the bioactive peptides. (Note, calculated masses agreed within 1 Da.)

| Peptide | Yield (%) | Mass/Da. |
|---|---|---|
| Δ0 | 77 | 1907 |
| Δ5 | 81 | 1791 |
| Δ45 | 83 | 1676 |

using helium sparged filtered water (0.1% TFA)/HPLC-grade acetonitrile (0.05% TFA) gradient. Acetonitrile was removed by rotary evaporation and the peptides were dried by lyophilization at Agriculture Canada in Kamloops, BC, Canada. The peptide masses were confirmed by MALDI-MS (Table 4) and determined to be >95% pure by analytical reversed-phase HPLC. Mass spectra and HPLC traces for the bioactive peptides can be found in the ESI.†

### Antimicrobial activity

Bacterial and fungal cultures were grown by inoculating Mueller Hinton broth with at least 10 separate colonies from either *Candida albicans*, *Salmonella typhimurium*, *Escherichia coli*, *Pseudomonas aeruginosa*, *Staphylococcus aureus*, or Methicillin-Resistant *Staphylococcus aureus* (MRSA). Cultures were grown to the same turbidity as a 0.5 McFarland Standard on an orbital shaker for approximately 30 min at 37 °C at 175 rpm. The bacterial and fungal broths were then diluted to the same turbidity as a 0.5 McFarland standard when necessary. These cultures were used to inoculate the media for the antimicrobial assay at a 200-fold final dilution. Peptides were dissolved in aqueous Mueller Hinton growth media at various concentrations. The cultures were inoculated with the bacterial and fungal species. The cultures were incubated at 37 °C for 24 h with constant shaking at 175 rpm. The optical densities of the cultures were then measured using a LKB·Novaspec II spectrophotometer (Pharmacia) at 600 nm ($OD_{600}$), where a 90% decrease in the $OD_{600}$ compared to the peptide-free controls was recorded as the minimum inhibitory concentration (MIC). The instrument was calibrated using broth as a blank. Bacterial/fungal cultures incubated without peptide were used as negative controls, whereas antimicrobial activity exhibited by indolicidin was taken as a positive control to demonstrate pathogen death with a known AMP. All samples were prepared in quadruplicate.

### Hemolytic activity

Anonymously donated blood was washed three times by centrifuging at 1000 rpm for 10 min at 4 °C and resuspending in phosphate-buffered saline (PBS 100 mM, pH 7.4). The buffy coat was removed after the first centrifugation. Samples were then brought back up to whole blood volume and diluted ten-fold to a final cell concentration of ~$5 \times 10^8$ cells $mL^{-1}$. Of this, 200 μL was added to 800 μL of sodium phosphate buffer (100 mM, pH 7.4) containing known peptide concentrations in 10-fold serial dilutions. Triton X-100 (1% final concentration) was added as a positive control, whereas sodium phosphate buffer (100 mM, pH 7.4) was used as a negative control. Samples were then inverted several times and incubated for one hour at 37 °C, with further inversions after 30 min. After incubation, samples were centrifuged at 14 000 rpm for 5 min, and the absorbance of the supernatant was measured at 541 nm to detect free hemoglobin in solution. The instrument was blanked against sodium phosphate buffer (100 mM, pH 7.4), and the amount of hemolysis exhibited by 1% Triton X-100 was taken to be 100% hemolysis (positive control). Thus, the percent hemolysis was taken to be:

$$\frac{(\text{Sample Absorbance}) - (\text{Negative Control Absorbance})}{(\text{Positive Control Absorbance})} \times 100\%$$

The minimum hemolytic concentration was taken to be the concentration of peptide that caused 100% hemolysis (relative to Triton X-100).

### Circular dichroism

All CD spectra were recorded on a JASCO J-810 at the UBC Laboratory of Molecular Biophysics. The J-810 had a computer-directed water bath set to 25 °C, a 400 W xenon lamp, and an IBM-compatible PC computer for data acquisition. Some of the parameter settings include: 0.1 nm step resolution, 2 nm bandwidth, and 50 nm $min^{-1}$ scanning speed. Each spectrum was an average of three scans subtracted from a reference background scan. Individual samples were run three times to ensure reproducibility. The peptides were monitored at their active concentrations respectively (~50 μM) in 50 mM sodium phosphate buffer (pH = 7.02) and in a 50% TFE solution to mimic the hydrophobic environment of the lipid membrane. A 2 mm quartz cuvette was used.

The raw spectra were normalized to a mean residue ellipticity [$\theta$] using the following equation:

$$[\theta] = \theta_{obs}/10lcn$$

where $\theta_{obs}$ is the observed ellipticity measured in millidegrees, $l$ is the path length in cm, $c$ is the peptide concentration in mol $L^{-1}$, and $n$ is the number of residues in the peptide. Errors were on average ± 5%.

### $^1$H nuclear magnetic resonance spectroscopy

Active derivatives were analyzed using a 500 MHz Bruker Avance AMIII 500 spectrometer and TXI probe with water suppression. Each sample was run at 298 K with 1024 scans and dissolved in 9 : 1 sodium phosphate buffer (50 mM, pH 7.0) to $D_2O$ with a final peptide concentration of ~1.5 mM.

### Apoptosis/necrosis cellular characterization

Bluegill Fibroblast ($BF_2$) cells were maintained in 15% MEM, which contained 12.5 mL Gibco MEM stock (containing inorganic salts, amino acids except glutamine, vitamins, glucose, succinic acid, and phenol red), 1 mL additional MEM vitamin stock, 1 mL L-glutamine (29.2 mg $mL^{-1}$), approximately 1 mL $NaHCO_3$ (7.5% w/v), 0.6 mL antibiotic/antimycotic (10 000 U of penicillin G; 10 000 μg $mL^{-1}$ streptomycin sulfate, 25 μg amphotericin β), 15 mL fetal calf serum, and deionized water up to a total volume of 100 mL. Cells were grown in the dark at room temperature in culture flasks.

To remove the adhered cells from the flasks, a preparation of trypsin–EDTA was used, which contained 10 mL trypsin–EDTA stock (0.5% trypsin, 5.3 mM $Na_4EDTA$), $NaHCO_3$ (7.5% w/v)



 

to neutralize, and deionized water up to a total volume of 100 mL. The cell suspension was then centrifuged at 3000 rpm for 5 min, and the supernatant was discarded. The pellet was resuspended in 15% MEM, and split into various tubes containing varying peptide concentrations. The cells were allowed to equilibrate for 30 min before visualization.

After equilibration, cells were treated with 50 μL of a double label staining solution containing annexin V bound to a fluorescent marker (AnnCy3) and 6-carboxyfluorescein diacetate (6-CFDA), and washed five times with 1X binding buffer to a final volume of 100 μL with centrifugation at 3000 rpm for 5 min between each wash. The cells were observed with brightfield microscopy and fluorescence microscopy (absorbance/emission 537/617 and 495/519 nm) with a Motic fluorescence microscope equipped with a 12 mega pixel digital camera.



## Acknowledgements

We would like to thank the Comprehensive University Enhancement Fund at Thompson Rivers University (TRU) for their financial support. Additional acknowledgements are given to the Departments of Physical and Biological Sciences at TRU, T. Hammer for setting up and servicing the instrumentation, C. Fardy for her assistance with ethics approval, blood donations, and laboratory technique instruction, D. Steinke for lyophilizing our samples at Agriculture Canada in Kamloops, BC, and lastly, F. Rosell and G. Mauk for the use of their Varian CARY Eclipse Spectrophotometer in the Life Sciences Center at the University of British Columbia.

## References

1 P. Courvalin, *J. Intern. Med.*, 2008, **264**, 4–16.
2 A. Peschel and H. Sahl, *Nat. Rev. Microbiol.*, 2006, **4**, 529–536.
3 R. Hancock and H. Sahl, *Nat. Biotechnol.*, 2006, **24**, 1551–1557.
4 M. Selsted, M. Novotny, W. Morris, Y. S. Tang and J. Cullor, *J. Biol. Chem.*, 1992, **267**, 4292–4295.
5 H. Schluesener, S. Radermacher, A. Melms and S. Jung, *J. Neuroimmunol.*, 1993, **47**, 199–202.
6 (*a*) C.-W. Tsai, N.-Y. Hsu, C.-H. Wang, C.-Y. Lu, Y. Chang, H.-H. Tsai and R.-C. Ruaan, *J. Mol. Biol.*, 2009, **392**, 837–854; (*b*) S.-M. Kim, J.-M. Kim, B. P. Joshi, H. Cho and K.-H. Lee, *Biochim. Biophys. Acta, Proteins Proteomics*, 2009, **1794**, 185–192.
7 (*a*) C. Subbalakshmi, V. Krishnakumari, R. Nagaraj and N. Sitaram, *FEBS Lett.*, 1996, **395**, 48–52; (*b*) C. Subbalakshmi, E. Bikshapathy, N. Sitaram and R. Nagaraj, *Biochem. Biophys. Res. Commun.*, 2000, **274**, 714–716.
8 P. Staubitz, A. Peschel, W. Nieuwenhuizen, M. Otto, F. Gotz, G. Jung and R. Jack, *J. Pept. Sci.*, 2001, **7**, 552–564.
9 T. Ryge, X. Doisy, D. Ifrah, J. Olsen and P. Hansen, *J. Pept. Res.*, 2004, **64**, 171–185.
10 (*a*) J. C. Y. Hsu and C. M. Yip, *Biophys. J.*, 2007, **92**, L100–L102; (*b*) C. Hsu, C. Chen, M. Jou, A. Lee, Y. Lin, Y. Yu, W. Huang and S. Wu, *Nucleic Acids Res.*, 2005, **33**, 4053–4064; (*c*) J. E. Shaw, J.-R. Alattia, J. E. Verity, G. G. Privé and C. M. Yip, *J. Struct. Biol.*, 2006, **154**, 42–58.
11 N. Sitaram, C. Subbalakshmi and R. Nagaraj, *Biochem. Biophys. Res. Commun.*, 2003, **309**, 879–884.
12 D. Lee, H. Kim, S. Kim, Y. Park, S. Park, S. Jang and K. Hahm, *Biochem. Biophys. Res. Commun.*, 2003, **305**, 305–310.
13 S. Aley, M. Zimmerman, M. Hetsko, M. Selsted and F. Gillin, *Infect. Immun.*, 1994, **62**, 5397–5403.
14 W. Robinson, B. McDougall, D. Tran and M. Selsted, *J. Leukocyte Biol.*, 1998, **63**, 94–100.
15 W. Wimley and S. White, *Nat. Struct. Biol.*, 1996, **3**, 842–848.
16 H. Boman, *J. Intern. Med.*, 2003, **254**, 197–215.
17 S. Nagpal, K. Kaur, D. Dinakar and D. Salunke, *Protein Sci.*, 2002, **11**, 2158–2167.
18 (*a*) W.C. Johnson Jr., *Proteins: Struct., Funct., Genet.*, 1990, **7**, 205–214; (*b*) R.W. Woody, *Methods Enzymol.*, 1995, **246**, 34–70; (*c*) G.D. Fasman, *Circular Dichroism and the Conformational Analysis of Biomolecules*, Plenum Press, New York, 1996.
19 K. Kuwajima, *Proteins: Struct., Funct., Genet.*, 1989, **6**, 87–103.
20 P.C. Kahn, *Methods Enzymol.*, 1979, **61**, 339–377.
21 A. Ladokhin, M. Selsted and S. White, *Biochemistry*, 1999, **38**, 12313–12319.
22 (*a*) J. Cavanagh, W.J. Fairbrother, A.G. Palmer III and N.J. Skelton, *Protein NMR Spectroscopy: Principles and Practice*, Academic Press, San Diego, 1996; (*b*) K. Wüthrich, *NMR of Proteins and Nucleic Acids*, Wiley, New York, 1986.
23 M.M. Bradford, *Anal. Biochem.*, 1976, **72**, 248–254.
24 H. Rink, *Tetrahedron Lett.*, 1987, **28**, 3787–3790.